Macromolecules
ARTICLE

Macromolecules **2010**, *43*, 1499–1506 **1499**
DOI: 10.1021/ma9023685

Biodegradable Poly(L-lactide)/Polyhedral Oligomeric Silsesquioxanes Nanocomposites: Enhanced Crystallization, Mechanical Properties, and Hydrolytic Degradation

Hong Pan and Zhaobin Qiu*

State Key laboratory of Chemical Resource Engineering, Beijing University of Chemical Technology, Beijing 100029, China

Received October 24, 2009; Revised Manuscript Received January 7, 2010

ABSTRACT: Biodegradable poly(L-lactide) (PLLA)/polyhedral oligomeric silsesquioxanes (POSS) nanocomposites were prepared in this work via solution and coagulation method at various POSS loadings in order to get a better dispersion of POSS in the PLLA matrix. Scanning electron microscopy observation indicates that POSS were nicely dispersed in the PLLA matrix. The overall crystallization rates are faster in the PLLA/POSS nanocomposites than in neat PLLA and increase with increasing the POSS loading; however, the crystallization mechanism and crystal structure of PLLA remain unchanged despite the presence of POSS. The storage modulus has been apparently improved in the PLLA/POSS nanocomposites with respect to neat PLLA, while the glass transition temperatures vary slightly between neat PLLA and the PLLA/POSS nanocomposites. It is interesting to find that the hydrolytic degradation rates have been enhanced obviously in the PLLA/POSS nanocomposites than in neat PLLA, which may be of great use and importance for the wider practical application of PLLA. The erosion mechanism of neat PLLA and the PLLA/POSS nanocomposites was further discussed.

Introduction

Poly(L-lactic acid) (PLLA) is a renewable, biodegradable, and biocompatible thermoplastic polymer, which has found practical application in the medical, agricultural, and general-purpose plastics fields.[1−4] However, its relatively poor mechanical properties, slow crystallization rate, and slow degradation rate have limited its further practical application. In order to overcome these disadvantages, copolymer synthesis, polymer blending, and reinforced composite methods have been developed.[5−10] The crystallization of PLLA has been enhanced in the presence of nucleating agents.[11−13] Tsuji et al. studied the nonisothermal melt crystallization of PLLA in the presence of various additives and found that the acceleration effects of additives on the overall crystallization of PLLA during cooling from the melt decreased in the following order: poly(D-lactic acid) > talc > C60 > montmorillonite > polysaccharides.[11] Recently, Tsuji et al. also found that the nucleation of PLLA is significantly enhanced in the presence of biodegradable poly(glycolic acid) (PGA) even at a PGA content as low as 0.1 wt %.[12] Zhou et al. found that carbonated hydroxyapatite acted as an efficient nucleating agent of PLLA, which enhanced the nucleation rate but reduced the spherulite growth rate at the same time.[13] The aforementioned studies mainly focus on the enhancement of crystallization of PLLA in the presence of nucleating agent; however, much less attention has been directed to the effect of the presence of nucleating agents on the mechanical properties and degradation behavior of PLLA.

Of particular interest is the recently developed nanocomposite technology consisting of carbon nanotubes (CNT) and layered silicate (clay) nanocomposites. The PLLA/CNT nanocomposites studies show that the crystallization of PLLA is accelerated, the hydrolytic degradation of PLLA is enhanced, and the mechanical, electrical, and thermal properties are improved after nanocomposites preparation.[14−17] The PLLA/clay nanocomposites represent an interesting class of materials due to the variety of structural forms possible to obtain (intercalated, exfoliated, and mixed), leading to significant improvement of the physical properties.[18−21]

The new three-dimensional nanofiller polyhedral oligomeric silsesquioxanes (POSS) have emerged as a new class of nanofillers for the preparation of higher performance nanostructured organic−inorganic composites in comparison with other inorganic nanofillers.[22,23] Until now, a number of works on POSS copolymers have been reported in the past few years;[24−32] however, polymer blending and nanocomposites preparation seem attractive owing to the advantages of being inexpensive and easy industrial implementation. A majority of polymers blended with POSS have been reported; among these studies most of them are traditional polymers such as polyethylene (PE), polypropylene (PP), poly(methyl methacrylate) (PMMA), poly(methylvinylsiloxane) (PMVS) elastomers, and polyimide (PI).[33−38]

It should be noted that biodegradable polymer nanocomposites comprising POSS by physical blending have not attracted much more consideration yet.[24−27] In our recent work,[39] a biodegradable PLLA/POSS nanocomposite was prepared by the solution casting method; however, POSS tended to agglomerate during slow solvent evaporation, leading to a relatively serious aggregation of POSS in the polymer matrix. Du et al. have recently developed a versatile solution and coagulation method that involves pouring a nanofillers/polymer suspension into an excess of nonsolvent and found that a good dispersion of single-wall carbon nanotubes could be achieved in the polymer nanocomposites.[40]

In this work, biodegradable PLLA/POSS nanocomposites were prepared via solution and coagulation method at various POSS loadings ranging from 1 to 10 wt % in order to get a better

*Corresponding author: e-mail qiuzb@mail.buct.edu.cn, Fax +86-10-64413161.

Published on Web 01/14/2010

dispersion of POSS in the PLLA matrix. Moreover, the influence of POSS on the crystallization, mechanical properties, and hydrolytic degradation of PLLA was investigated in detail with various techniques.

Experimental Section

PLLA ($M_w = 1.58 \times 10^5$) was kindly provided by Biomer Co., Germany. Octaisobutyl POSS was purchased from Sigma-Aldrich (Shanghai) Trading Co., Ltd. From now on, POSS was used in place of octaisobutyl POSS for brevity throughout the work. The PLLA/POSS nanocomposites were prepared through a solution and coagulation method with the addition of 1, 5, and 10 wt % POSS contents. For the fabrication of the nanocomposites, the following process was employed. First, appropriate amounts of PLLA and POSS were dissolved separately in chloroform. Second, the PLLA solution and the POSS solution were mixed together and stirred with sonication for 1 h. Third, the solution was precipitated into an excess of methanol, and then the filtering process was followed. Finally, the products were dried at 70 °C under vacuum for 3 days to remove the solvent completely. For brevity, the nanocomposites containing 1, 5, and 10 wt % of POSS are abbreviated as POSS-1, POSS-5, and POSS-10 from now on.

The morphology of the PLLA/POSS nanocomposites was observed using a Hitachi S-4700 scanning electron microscope (SEM). All specimens were coated with gold before examination.

Isothermal melt crystallization of neat PLLA and the PLLA/POSS nanocomposites was studied using a TA Instruments differential scanning calorimetry (DSC) Q100 with a Universal Analysis 2000. The samples were heated to 190 at 20 °C/min, held for 3 min to erase any thermal history, cooled to the desired crystallization temperature (T_c) at 40 °C/min, and held for a period of time until the isothermal crystallization was complete. The exothermal traces were recorded for the later data analysis.

An optical microscope (POM) (Olympus BX51) equipped with a temperature controller (Linkam THMS 600) was used to investigate the spherulitic morphology of neat PLLA and the PLLA/POSS nanocomposites.

Wide-angle X-ray diffraction (WAXD) experiments were performed on a Rigaku D/Max 2500 VB2t/PC X-ray diffractometer at room temperature in the range of 5°−40° with a scanning rate of 4°/min. The Cu Kα radiation ($\lambda = 0.154\,18$ nm) source was operated at 40 kV and 200 mA. The samples were first pressed into films with a thickness of around 0.6 mm on a hot stage at 190 °C and then transferred into a vacuum oven at 125 °C for 3 days.

For the dynamic mechanical analysis and hydrolytic degradation studies, the samples were molded into thick films on a hot press under a pressure of 10 MPa at 190 °C and further quenched into ice water. The obtained films were amorphous on the basis of the WAXD experiment. The thickness of the films was around 1 mm. Dynamic mechanical analysis (DMA) was performed on the samples of 42 mm × 8 mm × 1 mm in size using a dynamic mechanical analyzer from Rheometric Scientific Inc. under tension film mode in a temperature range of −10 to 150 °C at a frequency of 1 Hz and 3 °C/min.

The hydrolytic degradation of neat PLLA and its nanocomposites was carried out in sodium hydroxide (NaOH) solution (pH = 13) at 37 °C. The degradation of neat PLLA and its nanocomposites was determined by the variation of weight loss with degradation time. The weight loss coefficient W_{loss} (%) was evaluated by the following relationship: W_{loss} (%) = 100 × $(W_0 - W_{t\text{-dried}})/W_0$, where W_0 is the initial weight and $W_{t\text{-dried}}$ is the weight of sample subjected to hydrolytic degradation for time t and drying in vacuum. Three specimens were used to obtain the average W_{loss} values. Moreover, the hydrolytic degradation rate R was determined by the following relationship, i.e., $R = dW_{loss\text{-}t}/dt$, where $W_{loss\text{-}t}$ is the weight loss and t is the exposed time in NaOH solution. The molecular weight of the residual PLLA after degradation was measured by gel permeation chromatography (GPC) (Waters).

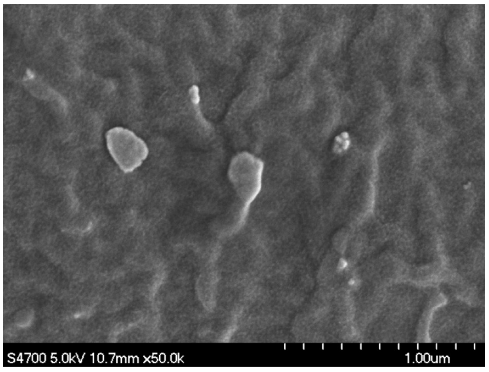

Figure 1. SEM images showing an overall morphology of fracture surface for a POSS-5 nanocomposite.

Results and Discussion

Morphology and Dispersion of POSS in the PLLA Matrix. It is well-known that the dispersion of POSS in the polymer matrix plays a dominant role of influencing the physical properties of biodegradable polymers. The fracture surface morphology of the PLLA/POSS nanocomposites samples was studied with SEM first. Figure 1 shows the SEM image of a POSS-5 sample as an example. It can be seen from Figure 1 that several white particles are randomly dispersed within the PLLA matrix as separate crystals. A fine dispersion of POSS is achieved in the PLLA matrix since the submicrometer aggregates with dimensions ranging from around 100 to 200 nm are found. Similar results are also found for the POSS-1 and POSS-10 samples. For brevity, the SEM images are not shown here. However, the dimension of the aggregates is about 200−400 nm when the PLLA/POSS nanocomposite was prepared via the solution casting method.[36] The formation of submicrometer aggregates of POSS particles indicates that there are somewhat compatibility between POSS and the PLLA matrix, which may be due to the modification of the isobutyl group of POSS. However, it is reported that in the PP/octaisobutyl POSS and low-density polyethylene (LLDPE)/octamethyl POSS nanocomposites the aggregation of POSS is serious, leading to microaggregates.[33,41] It should also be noted that the PLLA/POSS nanocomposites were prepared via the solution and coagulation method in this work while the LLDPE/octamethyl POSS and PP/octaisobutyl POSS nanocomposites were prepared via the melt compounding technique. The solution and coagulation method actually provides a better dispersion of POSS in the polymer matrix than the melt compounding method, which should be of great importance in studying the structure and properties relationship of biodegradable polymer/POSS nanocomposites.

Effect of POSS on the Isothermal Melt Crystallization of PLLA. It is of great interest to investigate the addition of POSS on the crystallization of PLLA in the PLLA/POSS nanocomposites. As introduced in the Experimental Section, the overall isothermal crystallization kinetics of neat PLLA and its nanocomposites was studied with DSC in a temperature range from 126 to 134 °C. The effect of the POSS loading on the isothermal melt crystallization of PLLA was studied first. Figure 2a shows the plots of relative crystallinity against crystallization time at 128 °C. It can be seen from Figure 2a that all these curves have the similar sigmoid shape. Furthermore, the corresponding crystallization time for the PLLA/POSS nanocomposites becomes shorter with increasing the POSS loading. For example, it took neat PLLA almost 60 min to complete crystallization at 128 °C; however, for the POSS-1, POSS-5, and POSS-10 nanocomposites, the time required to finish crystallization became only around 40, 31, and 21 min, respectively. It is clear that the addition of POSS enhances the isothermal melt crystallization

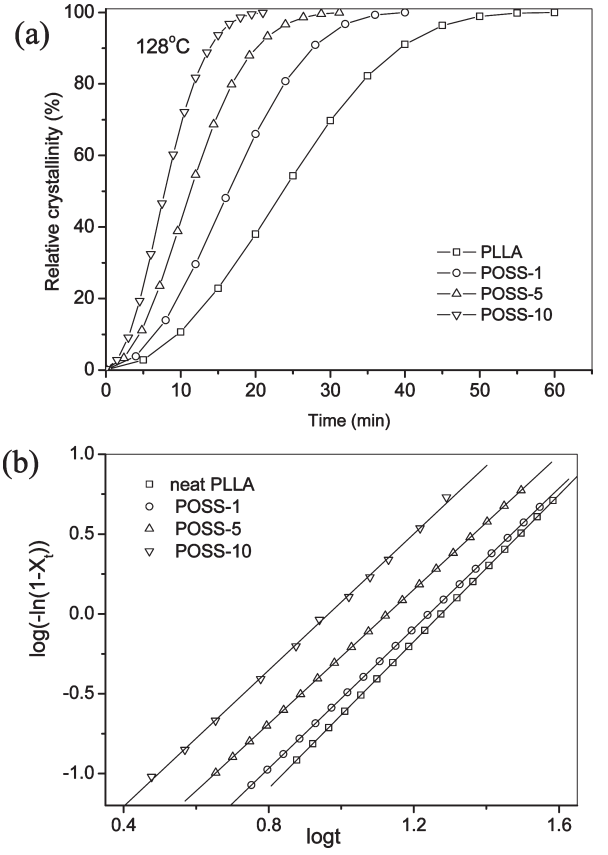

Figure 2. (a) Variation of relative crystallinity with crystallization time for neat PLLA and its nanocomposites at 128 °C and (b) the related Avrami plots.

of PLLA compared with neat PLLA; moreover, the crystallization rate is increased with increasing the POSS content.

The well-known Avrami equation is often used to analyze the isothermal crystallization kinetics;[42,43] it assumes that the relative degree of crystallinity develops with crystallization time t as

$$1 - X_t = \exp(-kt^n) \quad (1)$$

where X_t is the relative degree of crystallinity at time t, n is the Avrami exponent depending on the nature of nucleation and growth geometry of the crystals, and k is the crystallization rate constant involving both nucleation and growth rate parameters.[44,45] In the case of the DSC experiment, X_t at crystallization time t is defined as the ratio of the area under the exothermic curve between the onset crystallization time and the crystallization time t to the whole area under the exothermic curve from the onset crystallization time to the end crystallization time. Figure 2b shows the Avrami plots of neat PLLA and its nanocomposites crystallized at 128 °C as an example, from which the Avrami parameters n and k can be obtained from the slopes and the intercepts, respectively.

The obtained Avrami parameters of neat PLLA and its nanocomposites are summarized in Table 1, from which it can be seen that the average values of n are around 2.3 for neat PLLA and 2.2 for its nanocomposites at the investigated T_cs. The almost unchanged n suggests that the incorporation of POSS may not change the crystallization mechanism of PLLA in the PLLA/POSS nanocomposites.[45] Moreover, the values of k are also listed in Table 1.

However, it should be noted that it is difficult to compare the overall crystallization rate directly from the values of k

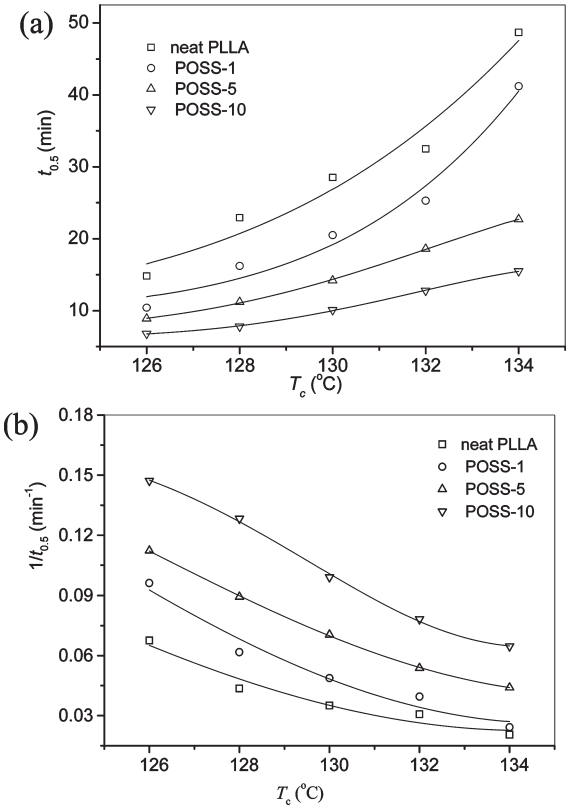

Figure 3. Temperature dependences of (a) $t_{0.5}$ and (b) $1/t_{0.5}$ for neat PLLA and its nanocomposites at various T_cs.

Table 1. Summary of Isothermal Crystallization Kinetics of Neat PLLA and the PLLA/POSS Nanocomposites at Different Crystallization Temperatures

samples	T_c (°C)	n	k (min^{-n})
neat PLLA	126	2.2	1.91×10^{-3}
	128	2.3	5.50×10^{-4}
	130	2.3	3.47×10^{-4}
	132	2.3	2.69×10^{-4}
	134	2.4	5.75×10^{-5}
POSS-1	126	2.2	3.63×10^{-3}
	128	2.2	1.18×10^{-3}
	130	2.2	4.94×10^{-4}
	132	2.1	8.13×10^{-4}
	134	2.4	1.07×10^{-4}
POSS-5	126	2.0	8.47×10^{-3}
	128	2.1	4.37×10^{-3}
	130	2.1	2.36×10^{-3}
	132	2.3	7.69×10^{-4}
	134	2.5	2.51×10^{-4}
POSS-10	126	2.2	1.02×10^{-2}
	128	2.1	8.12×10^{-3}
	130	2.2	3.25×10^{-3}
	132	2.2	2.34×10^{-3}
	134	2.2	1.62×10^{-3}

because the unit of k is min^{-n} and n is not constant. Thus, the half-time of crystallization $t_{0.5}$, the time required to achieve 50% of the final crystallinity of the samples, is introduced for the discussion of crystallization kinetics. The value of $t_{0.5}$ is calculated by the following equation:

$$t_{0.5} = \left(\frac{\ln 2}{k}\right)^{1/n} \quad (2)$$

Parts a and b of Figure 3 illustrate the variations of $t_{0.5}$ and $1/t_{0.5}$ with T_c for neat PLLA and its three nanocomposites,

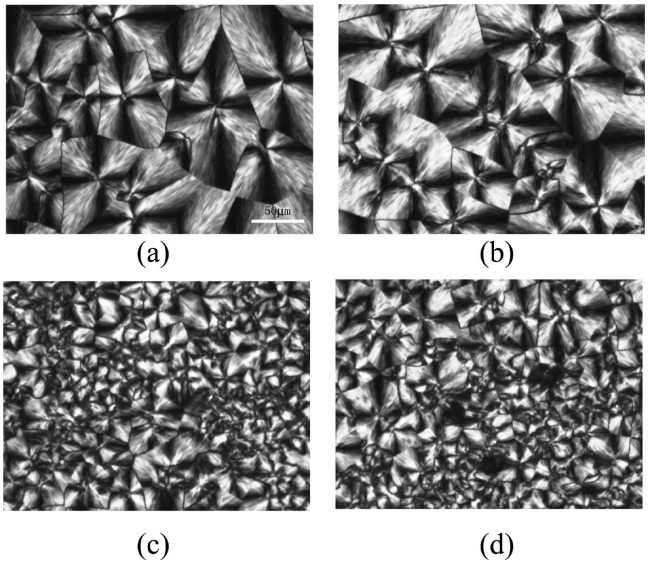

Figure 4. POM images of neat PLLA and its nanocomposites with different POSS loadings (with the same tool bar): (a) neat PLLA, (b) POSS-1, (c) POSS-5, and (d) POSS-10.

respectively, from which the effects of T_c and the POSS loading on the variation of overall crystallization rate can be obtained clearly. As shown in Figure 3, the values of $t_{0.5}$ increase while the values of $1/t_{0.5}$ decrease with increasing T_c for both neat PLLA and its nanocomposites. Such variations indicate that the overall isothermal crystallization rate decreases with increasing T_c due to the low supercooling in the chosen crystallization temperature range. In addition, the values of $t_{0.5}$ for the nanocomposites are smaller than those of neat PLLA at a given T_c, indicating again that the crystallization process of PLLA is accelerated after nanocomposite preparation, which may be due to the heterogeneous nucleation agent effect of POSS. It can also be seen from Figure 3b that the values of $1/t_{0.5}$ increase with increasing the POSS loading in the PLLA/POSS nanocomposites, suggesting that the POSS loading has a significant effect of accelerating the crystallization of PLLA. The DSC results reported herein are consistent with the spherulitic morphology and growth studies in the following section.

Spherulitic morphology of neat PLLA and its nanocomposite was studied with POM. Figure 4 shows the spherulitic morphology of neat PLLA and its nanocomposites isothermally crystallized at 125 °C. It can be seen from Figure 4a that the well-developed spherulites grow to a size of about 50 μm in diameter, and the boundaries can be seen clearly for neat PLLA. Parts b, c, and d of Figure 4 illustrate the POM images of the nanocomposites with the POSS loading from 1 to 10 wt %. It is obvious that the size of PLLA spherulites becomes smaller, and the spherulites boundaries are obscurer with increasing the POSS content. The nucleation density of PLLA spherulites increases in the presence of POSS in the PLLA/POSS nanocomposites because of their nucleation agent effect. In conclusion, the presence of POSS and their contents in the PLLA matrix have a significant influence on the spherulitic morphology and the overall crystallization process of PLLA.

WAXD experiments were performed to investigate the effect of the addition of POSS on the crystal structure of PLLA in the PLLA/POSS nanocomposites. Three crystal modifications, including α, β, and γ forms, have been reported for PLLA.[46,47] Crystallization from the melt usually leads to α form, which is the most common polymorph.

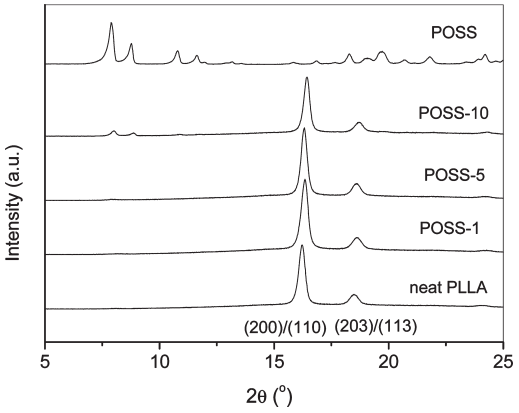

Figure 5. WAXD patterns of neat PLLA and its nanocomposites.

Recently, a new crystal modification α′ has also been found.[48−50] The formation of the metastable α′-form crystals of PLLA is kinetically preferential, while that of the thermally stable α-form crystals is thermodynamically favored. It has been found that the disorder α′ and order α phases are formed at low (T_c < 100 °C) and high (T_c > 120 °C) temperatures, respectively. In the previous section, the isothermal crystallization kinetics of neat PLLA and its nanocomposites was studied in the temperature range of 126−134 °C; thus, it is believed that they all crystallized in α form in this work. As POSS appears to act as an effective nucleating agent for PLLA, it would be of great interest to analyze whether it has any effect in enhancing nucleation of either α or α′ form. Such work needs further investigation.

In this work, the samples for the WAXD measurements were crystallized at 125 °C; therefore, neat PLLA and its nanocomposites crystallize in α form. In Figure 5, the presence of a number of strong diffraction peaks shows that POSS are highly crystalline. For neat PLLA, two sharp characteristic diffraction peaks are shown at 16.25° and 18.57°, corresponding to (200)/(110) and (203) planes, respectively.[51] Moreover, the nanocomposites also exhibit nearly the same diffraction peaks at the same locations, indicating that incorporating with POSS does not modify the crystal structure of PLLA. In addition, the characteristic diffraction peaks of POSS at around 7.89° and 8.77° appear in the POSS-10 nanocomposite, suggesting that POSS exist as the separate crystals or POSS particles are able to crystallize when they are dispersed in the PLLA matrix. The appearance of the diffraction peaks of POSS in the POSS-10 nanocomposites may be related to the fact that the agglomeration and crystallization of POSS particles are easier at higher concentration. However, no clear POSS characteristic peaks are found for the POSS-1 and POSS-5 nanocomposites probably due to the low POSS contents. In brief, the crystal structure of PLLA remains unchanged despite the addition of POSS in the PLLA/POSS nanocomposites.

Dynamic Mechanical Analysis. In the aforementioned sections, it is found that the crystallization of PLLA is enhanced after nanocomposites preparation. In this section, the effect of POSS on the dynamic mechanical properties of PLLA was studied. Parts a and b of Figure 6 show the temperature dependence of storage modulus (E') and tan δ, the ratio of loss modulus to storage modulus, of neat PLLA and the PLLA/POSS nanocomposites, respectively. From Figure 6a, a considerable increase of the storage modulus is found after the incorporation of POSS at low temperature in the glass state (0−60 °C), indicating that the addition of POSS particles induces a reinforcement effect. For example,

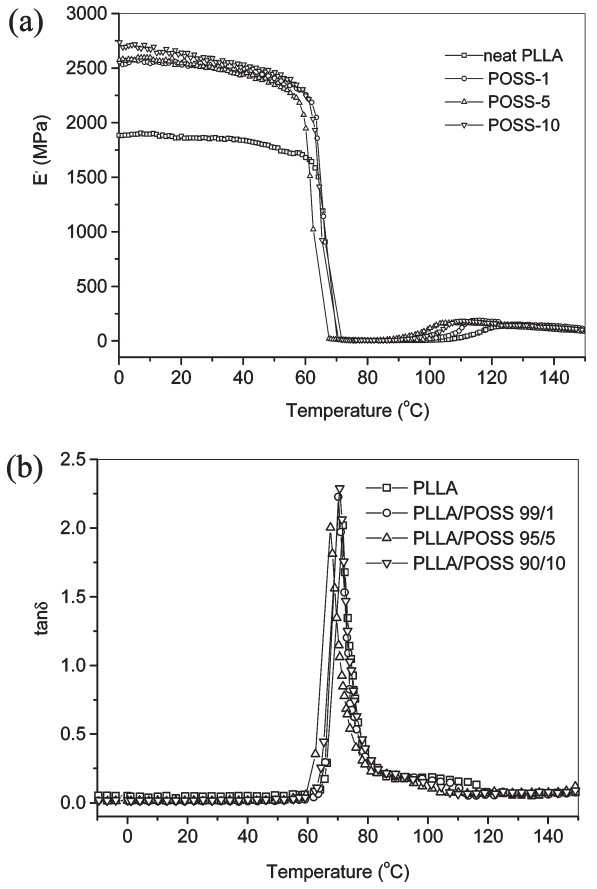

Figure 6. Temperature dependence of (a) storage modulus and (b) tan δ for neat PLLA and its nanocomposites.

the value of E' is around 1875 MPa for neat PLLA at 20 °C, which increases to around 2527, 2544, and 2640 MPa, respectively, with increasing the POSS loading from 1 to 10 wt %. It should be noted that the increase in E' is significant with the POSS loadings from 0 to 1 wt %; however, the difference is slight with further increasing POSS loading from 1 to 10 wt % in the PLLA matrix, indicating that such effect is more pronounced at lower POSS content. The significant improvement in E' may be ascribed to the combined effect of high performance and fine dispersion of POSS. A similar phenomenon was also found in the LLDPE/POSS nanocomposites.[41] It was found that the modulus of LLDPE/POSS nanocomposites was improved after the incorporation of POSS. Furthermore, it is seen that both neat PLLA and the PLLA/POSS nanocomposites exhibit a sharp reduction of elastic modulus around 70 °C, corresponding to the glass transition of PLLA. It should be noted that E' of POSS-5 starts to decrease at a lower temperature compared to other samples. The exact reason is still uncertain, and further investigation is currently underway. In addition, the storage modulus difference between neat PLLA and the PLLA/POSS nanocomposites is very small and tends to zero in the temperature range of 70−150 °C, suggesting that the nanocomposites stiffness become matrix dependent at the rubbery state. From Figure 6b, the glass transition temperatures for both neat PLLA and the PLLA/POSS nanocomposites are estimated to be around 70 °C, indicating that the presence of POSS does not significantly influence the segmental motion of PLLA in the nanocomposites.

Hydrolytic Degradation. In the above sections, the effects of POSS on the crystallization behavior and dynamic mechanical properties of PLLA were studied in the PLLA/POSS nanocomposites. In this section, the effect of POSS on the hydrolytic degradation of PLLA in the nanocomposites was further investigated. Figure 7 shows the variation of weight loss of neat PLLA and its nanocomposites with exposed time during hydrolysis test. The values of weight loss increase with prolonging exposed time for both neat PLLA and its nanocomposites. As shown in Figure 7, mass loss starts from the beginning of each degradation experiment and shows almost linear variation of weight loss with exposed time until 28 days. Since the weight loss shows almost linear increase with hydrolytic degradation time, the hydrolytic degradation rates of neat PLLA and the PLLA/POSS nanocomposite are obtained from the slopes of the plots of variation of weight loss with hydrolytic degradation time. For neat PLLA, the hydrolytic degradation rate is around 1.76%/day; however, the hydrolytic degradation rates are increased to be around 1.94, 2.57, and 3.31%/day for the PLLA/POSS nanocomposites with increasing the POSS loading from 1 to 10 wt %. It is obvious that the nanocomposites degrade faster than neat PLLA, indicating the loading of POSS accelerates the hydrolytic degradation of PLLA in the nanocomposites; moreover, the hydrolytic degradation rate increases with increasing the POSS content. The results that polymer degrades faster in the polymer nanocomposites than in neat polymer have also been recently reported in the literature.[52,53] Sinha Ray and Paul have reported that the biodegradation and hydrolytic degradation of the PLLA composites containing organo-modified montmorillonite (MMT) and unmodified MMT (microcomposites) are faster than those of neat PLLA.[52,53]

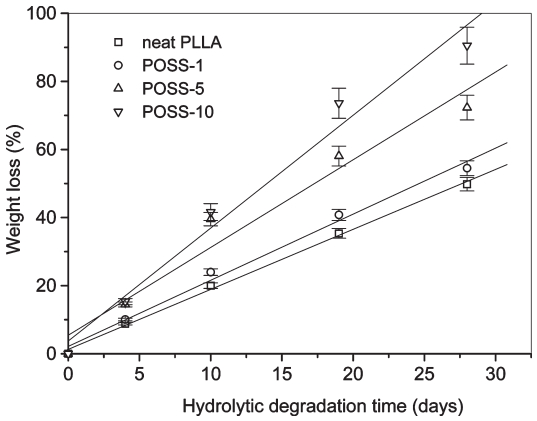

Figure 7. Variation of weight loss with hydrolytic degradation time for neat PLLA and its nanocomposites.

The weight-average molecular weight (M_w) of neat PLLA and the PLLA/POSS nanocomposites were also studied during the hydrolytic degradation process. It is found that the M_w values remain almost unchanged for both neat PLLA and its nanocomposites during the hydrolytic degradation process. The almost unchanged M_w indicates that no significant chain scission occurred for both neat PLLA and the PLLA/POSS nanocomposite during the hydrolytic degradation process. Many factors may affect the degradation of aliphatic polyesters, such as pH, temperature, morphology, crystallinity, erosion mechanism, etc. In the present work, the same environmental conditions, i.e., pH and temperature, were used in studying the hydrolytic degradation; furthermore, both neat PLLA and the PLLA/POSS nanocomposite samples are amorphous prior to hydrolytic degradation, suggesting that crystallinity is not a factor influencing the hydrolytic degradation of PLLA in the

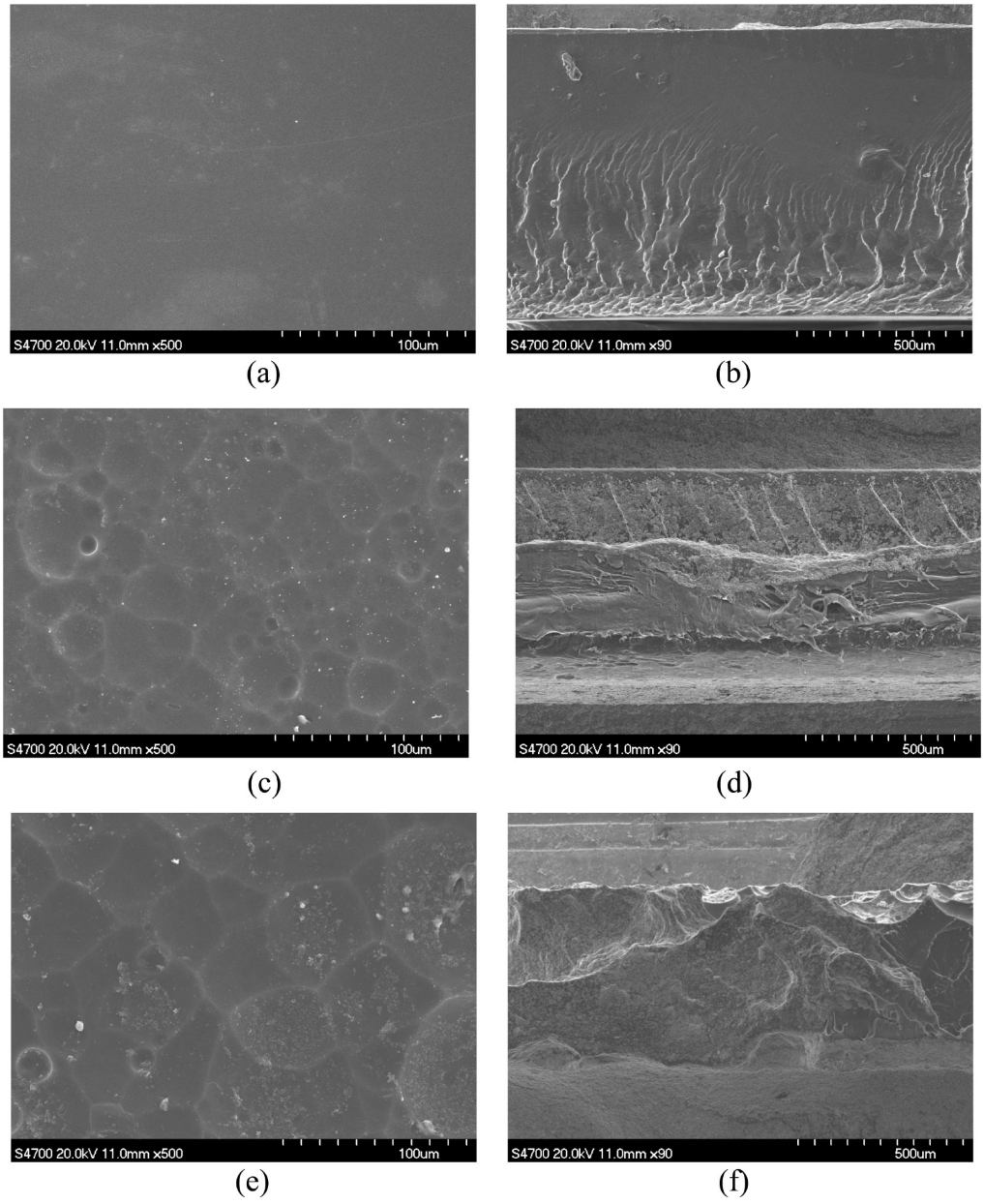

Figure 8. SEM images showing the morphology of surface and cross-section for neat PLLA and POSS-5 samples: (a) surface of neat PLLA before degradation; (b) cross section of neat PLLA before degradation; (c) surface of neat PLLA after a degradation of 19 days; (d) cross section of neat PLLA after a degradation of 19 days; (e) surface of POSS-5 after a degradation of 19 days; (f) cross section of POSS-5 after a degradation of 19 days.

present work. It is well-known that degradation of polymers can be mainly classified into two typical types, i.e., surface eroding and bulk eroding ones. In the case of ideal bulk erosion, material is lost from the entire polymer volume; moreover, the erosion rate depends on the total amount of material and generally decreases as material is depleted. Therefore, the length of time the polymer persists can be altered by changes in chemical composition but not by the size or shape of the materials. In the case of surface erosion, material is lost from the polymer matrix exterior surface; moreover, the erosion rate is directly proportional to external surface area and remains constant as the slab becomes progressively thinner. For a surface-eroding polymer, the erosion rate is essentially constant until the polymer is completely eroded; therefore, control of the time span the polymer persists can be achieved by not only changing its chemical properties but also adjusting the dimensions and shape of the material.[54−58] Therefore, it is interesting to investigate further the erosion mechanism of neat PLLA and its nanocomposites during the hydrolytic degradation process. The almost unchanged hydrolytic degradation rates and molecular weight suggest that the hydrolytic degradation of neat PLLA and the PLLA/POSS nanocomposite may proceed via the surface erosion mechanism; thus, only the surface of the samples was eroded while the internal remained almost unchanged during the degradation process. Moreover, the almost unchanged molecular weight indicates that there is no evident chain scission during hydrolytic degradation.

In order to investigate the erosion mechanism, the surface and cross-section images of neat PLLA and the PLLA/POSS nanocomposites were studied with SEM. Parts a−d of Figure 8 illustrate the SEM images of neat PLLA before and after hydrolytic degradation. Figure 8a,b shows the surface and cross-section images of neat PLLA prior to hydrolytic degradation, while Figure 8c,d shows the surface

and cross-section images of neat PLLA after a hydrolytic degradation of 19 days. It is obvious from parts a and c of Figure 8 that the surface of neat PLLA is very smooth before degradation while that of degraded neat PLLA becomes blemished and appears cell-like spots structure. On the contrary, no apparent morphology change takes place in the inside of the films from the cross-section images study as shown in parts b and d of Figure 8; however, the film thickness of neat PLLA decreased after a hydrolytic degradation, indicating again that the hydrolytic degradation of neat PLLA may proceed via surface erosion mechanism. Similarly, the morphological changes of the surface and cross-section images for the PLLA/POSS nanocomposites were also studied for comparison. Parts e and f of Figure 8 show the corresponding surface and cross-section SEM images of a POSS-5 nanocomposite after a hydrolytic degradation of 19 days as an example. The surface of the POSS-5 nanocomposite shown in Figure 8e is rougher than that of neat PLLA shown in Figure 8c after a hydrolytic degradation of 19 days; moreover, the films tend to become thinner in the POSS-5 nanocomposite than in neat PLLA if we compare the cross-section images shown in Figure 8d,f after a hydrolytic degradation. The variation of the film thickness suggests that surface erosion still occurred despite the presence of POSS in the PLLA/POSS nanocomposite; furthermore, increasing the POSS loading accelerates the hydrolytic process. Similar results are also found in the POSS-1 and POSS-10 samples. For brevity, the results are not shown here.

From the above studies, it can be deduced that the hydrolytic degradation of both neat PLLA and the PLLA/POSS nanocomposites occurred at the surface of the films. Such results are consistent with the previous research conclusion that the erosion of PLLA process proceeds via surface erosion in alkaline solution.[59−61] During the hydrolytic degradation, both the weight and thickness of the films decreased with time, while the molecular weight remained almost unchanged. The hydrolytic degradation rates are faster in the PLLA/POSS nanocomposites than in neat PLLA and increase with the POSS loading; however, the exact reason is still unknown and needs further investigation.

Conclusions

Biodegradable PLLA/POSS nanocomposites were prepared via the solution and coagulation method at various POSS loadings from 1 to 10 wt %. The crystallization, dynamic mechanical properties, and hydrolytic degradation of neat PLLA and the PLLA/POSS nanocomposites were investigated in detail with various techniques. The following conclusions were obtained:

1. SEM observation indicates that POSS were nicely dispersed in the PLLA matrix, forming submicrometer aggregates at a size of around 100−200 nm. The nice distribution and the size of the aggregates of POSS suggest that the solution and coagulation method is an efficient method for preparing POSS containing polymer nanocomposites.

2. Isothermal melt crystallization studies show that the overall crystallization rates are faster in the PLLA/POSS nanocomposites than in neat PLLA and increase with increasing the POSS loading; however, the crystallization mechanism and crystal structure of PLLA remain unchanged despite the presence of POSS.

3. Compared with neat PLLA, the incorporation of POSS has improved apparently the storage modulus of the PLLA/POSS nanocomposites, with this effect being more pronounced at lower POSS content; however, the glass transition temperatures vary slightly between neat PLLA and the PLLA/POSS nanocomposites. The exciting result of this work is that the hydrolytic degradation rates have been enhanced obviously in the PLLA/POSS nanocomposites than in neat PLLA, which may be of great use and importance for the wider practical application of PLLA. The erosion mechanism of neat PLLA and the PLLA/POSS nanocomposites was further discussed, and the hydrolytic degradation of neat PLLA and the PLLA/POSS nanocomposites may proceed via surface erosion.

Acknowledgment. Thanks are due to Biomer, Germany, for kindly providing the PLLA samples. Part of this work is financially supported by the National Natural Science Foundation, China (20774013 and 20974012), Program for New Century Excellent Talents in University (NCET-06-0101), Program for Changjiang Scholars and Innovative Research Team in University (IRT0706), and the projects of Polymer Chemistry and Physics, Beijing Municipal Commission of Education (XK100100640).

References and Notes

(1) Garlotta, D. *Polym. Environ.* **2001**, *9*, 63.
(2) Bogaert, J.; Coszac, P. *Macromol. Symp.* **2000**, *153*, 287.
(3) Drumright, R.; Gruber, P.; Henton, D. *Adv. Mater.* **2000**, *12*, 1841.
(4) Ikada, Y.; Tsuji, H. *Macromol. Rapid Commun.* **2000**, *21*, 117.
(5) Lu, J.; Qiu, Z.; Yang, W. *Polymer* **2007**, *48*, 4196.
(6) Wu, C.; Liao, H. *Polymer* **2008**, *48*, 4449.
(7) Chang, J.; An, Y.; Sur, G. *J. Polym. Sci., Part B: Polym. Phys.* **2003**, *41*, 94.
(8) Fukuda, N.; Tsuji, H. *J. Appl. Polym. Sci.* **2005**, *96*, 190.
(9) Thostenson, T.; Ren, Z.; Chou, T. *Compos. Sci. Technol.* **2001**, *61*, 1899.
(10) http://www.nanoclay.com.
(11) Tsuji, H.; Takai, H.; Fukuda, N.; Takikawa, H. *Macromol. Mater. Eng.* **2006**, *291*, 325.
(12) Tsuji, H.; Tashiro, K.; Bouapao, L.; Narita, J. *Macromol. Mater. Eng.* **2008**, *293*, 947.
(13) Zhou, W.; Duan, B.; Wang, M.; Cheung, W. *J. Appl. Polym. Sci.* **2009**, *113*, 4100.
(14) Zhao, Y.; Qiu, Z.; Yang, W. *J. Phys. Chem. B* **2008**, *112*, 16461.
(15) Zhang, D.; Kandadai, M.; Cech, J.; Roth, S.; Curran, S. *J. Phys. Chem. B* **2006**, *110*, 12910.
(16) Shieh, T.; Liui, L. *J. Polym. Sci., Part B: Polym. Phys.* **2007**, *45*, 1870.
(17) Kim, S.; Park, B.; Yoon, J.; Jin, H. *Eur. Polym. J.* **2007**, *43*, 1729.
(18) Ogata, N.; Jimenez, G.; Kawai, H.; Ogihara, T. *J. Polym. Sci., Part B: Polym. Phys.* **1997**, *35*, 389.
(19) Shina Ray, S.; Yamada, K.; Okamoto, M.; Ueda, K. *Nano Lett.* **2002**, *2*, 1093.
(20) Pluta, M.; Paul, M.; Alexandre, M.; Dubois, P.; Galeski, A. *J. Appl. Polym. Sci.* **2002**, *86*, 1497.
(21) Maiti, P.; Yamada, K.; Okamoto, M.; Ueda, K.; Okamato, K. *Chem. Mater.* **2002**, *14*, 4654.
(22) Harrison, P. *J. Organomet. Chem.* **1997**, *542*, 141.
(23) Li, G.; Wang, L.; Ni, H.; Pittman *J. Inorg. Org. Polym.* **2001**, *11*, 123.
(24) Ni, Y.; Zheng, S. *J. Polym. Sci., Part A: Polym. Chem.* **2007**, *45*, 1247.
(25) Liu, Y.; Yang, X.; Zhang, W.; Zheng, S. *Polymer* **2006**, *47*, 6814.
(26) Ni, Y.; Zheng, S. *J. Polym. Sci., Part B: Polym. Phys.* **2007** *45*, 2201.
(27) Goffin, A.; Duquesne, E.; Moins, S.; Alexandre, M.; Dubois, P. *Eur. Polym. J.* **2007**, *43*, 4103.
(28) Lin, H.; Wu, S.; Huang, P.; Huang, C.; Kuo, S.; Chang, F. *Macromol. Rapid Commun.* **2008**, *27*, 1550.
(29) Kim, B.; Mather, P. *Macromolecules* **2006**, *39*, 9253.
(30) Choi, J.; Kim, S.; Laine, R. *Macromolecules* **2004**, *37*, 99.
(31) Lee, Y.; Kuo, S.; Huang, W.; Lee, H.; Chang, F. *J. Polym. Sci., Part B: Polym. Phys.* **2004**, *42*, 1127.
(32) Zheng, L.; Farris, R.; Coughlin, E. *Macromolecules* **2001**, *34*, 8034.
(33) Fina, A.; Tabuani, D.; Frache, A.; Camino, G. *Polymer* **2005**, *46*, 7855.
(34) Lee, Y.; Huang, J.; Kuo, S.; Chang, F. *Polymer* **2005**, *46*, 10056.
(35) Zhao, Y.; Schiraldi, D. *Polymer* **2005**, *46*, 11640.
(36) Sharon, Y.; Cohen, R.; Boyce, M. *Polymer* **2007**, *48*, 1410.

(37) Zhang, Y.; Lee, S.; Yoonessi, M.; Liang, K.; Pittman, C. *Polymer* **2006**, *47*, 2984.
(38) Kopesky, E.; McKinley, G.; Cohen, R. *Polymer* **2006**, *47*, 299.
(39) Pan, H. Master Dissertation, Beijing University of Chemical Technology, Beijing, **2009**.
(40) Du, F.; Fischer, J.; Winey, K. *J. Polym. Sci., Part B: Polym. Phys.* **2003**, *41*, 3333.
(41) Hato, M.; Sinha Ray, S.; Luyt, A. *Macromol. Mater. Eng.* **2008**, *293*, 752.
(42) Avrami, M. *J. Chem. Phys.* **1940**, *8*, 212.
(43) Avrami, M. *J. Chem. Phys.* **1941**, *9*, 177.
(44) Kamal, M.; Chu, E. *Polym. Eng. Sci.* **1983**, *23*, 27.
(45) Wunderlich, B. In *Macromolecular Physics*; Academic Press: New York, 1976; Vol. *2*, p 147.
(46) De Santis, P.; Kovacs, A. *Biopolymers* **1968**, *6*, 299.
(47) Kawai, T.; Rahman, N.; Matsuba, G.; Nishida, K.; Kanaya, T.; Nakano, M.; Okamoto, H.; Kawada, J.; Usuki, A.; Honma, N.; Nakajima, K.; Matsuda, M. *Macromolecules* **2007**, *40*, 9463.
(48) Qiu, X.; Redwine, D.; Gobbi Anuttra Nuamthanom, G.; Rinaldi, P. *Macromolecules* **2007**, *40*, 6879.
(49) Pan, P .; Zhu, B.; Kai, W.; Dong, T.; Inoue, Y. *Macromolecules* **2008**, *41*, 4296.
(50) Di Lorenzo, M. *Eur. Polym. J.* **2005**, *41*, 569.
(51) Hoogsteen, W.; Postema, A.; Pennings, A.; Ten Brinke, G.; Zugenmaier, P. *Macromolecules* **1990**, *23*, 634.
(52) Sinha Ray, S.; Yamada, K.; Okamoto, M.; Ueda, K. *Macromol. Mater. Eng.* **2003**, *288*, 203.
(53) Paul, M.; Decourt, C.; Alexandre, M.; Degee, P.; Monteverde, F.; Dubois, P. *Polym. Degrad. Stab.* **2005**, *87*, 535.
(54) Tamada, J.; Langer, R. *Proc. Natl. Acad. Sci. U.S.A.* **1993**, *90*, 552.
(55) Gophferich, A. *Biomaterials* **1996**, *17*, 103.
(56) Grizzi, I.; Garreau, H.; Li, S.; Vert, M. *Biomaterials* **1995**, *16*, 305.
(57) Burkersrodaa, F.; Schedl, L.; Göpferich, A. *Biomaterials* **2002**, *23*, 4221.
(58) Doi, Y.; Kanesawa, Y.; Kunioka, M.; Saito, T. *Macromolecules* **1990**, *23*, 26.
(59) Tsuji, H.; Ikada, Y. *J. Polym. Sci., Part A: Polym. Chem.* **1998**, *45*, 59.
(60) Tsuji, H.; Ishida, T. *J. Appl. Polym. Sci.* **2003**, *87*, 1628.
(61) Fukuda, N.; Tsuji, H. *J. Appl. Polym. Sci.* **2005**, *96*, 190.